CONF-850173--3

DE85 018100

CONF-850173--3

Contribution to the XXIII International Meeting on Nuclear Physics
BORMIO, January 21-26, 1985

GAMMA-SPECTROMETRY WITH COMPTON SUPPRESSED DETECTORS ARRAYS

C. Schück and F. Hannachi
Laboratoire S. Rosenblum, CSNSM 91406 ORSAY, FRANCE

R. Chapman, J.C. Lisle, J.N. Mo and E. Paul
Schuster Laboratory, Univ. of Manchester, MANCHESTER, U.K.

D.J. G. Love, P.J. Nolan and A.H. Nelson
University of Liverpool, LIVERPOOL, U.K.

P.M. Walker
Daresbury Laboratory, WARRINGTON, U.K.

Y. Ellis-Akovali and N.R. Johnson
Oak-Ridge National Laboratory, OAK-RIDGE, TN 37830, U.S.A.

N. Bendjaballah
CEN-CDTB, B.P. 1017 ALGER-Gare, ALGERIA

R.M. Diamond, M.A. Deleplanque, F.S. Stephens, G. Dines and J. Draper
Lawrence Berkeley Laboratory, BERKELEY CA 94720, U.S.A.

Recent results of experiments performed with two different Compton-suppressed detectors arrays in Daresbury and Berkeley (^{163,164}Yb and ^{154}Er respectively), are presented together with a brief description of the national french array presently under construction in Strasbourg.

I - INTRODUCTION

There is now a number of existing or funded multi-Ge-detectors arrays associated with Anti-Compton suppressors. The use of Compton suppression shields improves by an order of magnitude the fraction of useful (Peak/Total) events in γ-γ coincidence measurements. Discrete lines spectroscopy (and useful "semi-continuum" Eγ-Eγ correlations) can therefore be extended up to a region of spins which could recently be reached only through studies in the continuum. In the high spin range ($30\hbar < I < 60\hbar$) important changes of shape and structure are predicted and it is particularly interesting to study the interplay between collective and single particle excitation modes in that region.

Most of these multi-detector arrays are (or will be) associated with an inner core of detectors providing the selection of an entrance channel by Sum Energy/Multiplicity determination. A number of very successfull results have already been obtained with the first device of this kind, TESSA[1], operating in Daresbury since early 1983. The actual TESSA2 consists of an array of six Ge detectors, each of them being surrounded with a NaI (Tl) suppression shield, associated with a compact inner core of 50 BGO scintillators. It will soon be transformed as TESSA3 with 12 Ge detectors equiped with BGO Anti-Compton shields. The next generation (POLYTESSA)[2] will include 20 Ge detectors and will be able to accomodate 30. The Berkeley array[3] is the first one where BGO Anti-Compton shields have been used. The outer ball is now completed with 21 Compton suppressed Ge detectors and will, in the next stage, be associated with an inner core of 40 BGO elements. Other arrays are in different phases of development in Germany (OSIRIS), Argonne, MSU-Pittsburg, Oak Ridge, as well as the canadian "8π-spectrometer", the scandinavian NORDBALL and the french "Chateau de Cristal" (this array will be briefly described in section IV).

For all these devices, the Compton-shields (NaI, BGO, BaF2) dimensions are optimised in order to provide a ratio of useful Peak/Total events ~ 0.5-0.6 in the single spectra. The main factors that determines the rate of coincidence events acquisition is (i) the number

of Ge detectors, (ii) the distance from target to detectors. In the Daresbury and Berkeley arrays typical different choices were made with respect to the latter dimension (d = 27 cm and 14 cm respectively). One has then to take into consideration the Doppler broadening of the γ-rays. The Doppler smearing is due to the change in energy across a detector of γ-rays emitted by fast recoiling nuclei (v/c ~ 2% to 3% in a typical Heavy Ion reaction). For collective rotors (such as rare earth nuclei with N $\geq$ 90) the nucleus deexcites rapidly by enhanced E2 transitions. In the non-collective case the nucleus radiates both its energy and angular momentum relatively slowly. That is the situation for the island of nuclei near the Z = 64, N = 82 doubly closed shell, which have large deexcitation times compared to the picosecond. Such recoil nuclei can be stopped into a high density backing (lead or gold) in about 1 psec. Therefore, γ-rays emitted by states with large half-lives compared to the picosecond will show no Doppler broadening if backed target are used.

In such arrays as TESSA, nuclei which behave as collective rotors up to very high spins can be studied by using thin targets. The Doppler smearing at 1 MeV will be less than the resolution of the Ge detectors. Such a case of collective well deformed rotors is presented in section II.

The Berkeley array, with d = 14 cm, thus allowing a very high counting rate and the possibility of using triple coincidences, is particularly well adapted for studying a typical non-collective rotor as ^{154}Er which will be presented in section III.

II - COLLECTIVE ROTORS OF THE RARE EARTH REGION : ^{163,164}Yb

The deformation parameters for the low-lying states of ^{163}Yb and ^{164}Yb are ϵ_2 = 0.25, ϵ_4 = 0.005 and γ = 0° according to Lund calculations[4] and are expected to remain reasonably constant up to I ~ 50h. These nuclei can thus be considered as well deformed prolate rotors for the range of spins available in the following experiments. For such a deformation the first proton crossing is not predicted to occur below $\hbar\omega$ = 0.5 MeV and therefore the quasi-neutron configurations can be observed over a large range of frequencies.

The experiment described in this section was performed by an Orsay, Manchester, Liverpool, Daresbury, Oak-Ridge and Algiers collaboration.

^{163,164}Yb have been produced using the reaction ^{124}Sn(^{44}Ca,xn), the 194 MeV ^{44}Ca beam being provided by the Daresbury tandem accelerator. Three thin stacked ^{124}Sn targets, each of 400μg/cm^2 thickness, were used. The γ-rays were detected with the TESSA2 facility[1]. Coincidence events for which at least two Ge detectors fired were recorded on magnetic tape together with the sum energy and fold. A total of 24.10^6 events were recorded.

Gates on both the sum energy and the fold allowed a selection of the 4n and 5n channels during the data processing. Typical spectra obtained by setting windows on the higher energy transitions in the appropriate band for both 4n and 5n channels are shown in fig. 1. The resulting level schemes for ^{163}Yb and ^{164}Yb (which had previously been studied by a Lund N.B.I. collaboration[5,6] using an oxygen beam), are presented in fig. 2 and fig. 3 respectively. In ^{163}Yb the yrast band has been tentatively extended up to $I^\pi = 65/2^+$ and the (−,+) band up to $I^\pi = 61/2^-$. In ^{164}Yb the yrast band has been observed up to the $I^\pi = 34h$ member and two negative parity bands have been seen up to $I^\pi = 31^-h$ and 32^-h respectively. The different bands are labelled by their parities and signatures.

The total angular momentum aligned along the rotation axis

$$I_x = \sqrt{(I + 1/2)^2 - K^2}$$

has been plotted in fig. 4 and fig. 5 for different rotational bands in ^{163}Yb and ^{164}Yb respectively. It may be parametrized in terms of an intrinsic aligned angular momentum i and a variable momentum of inertia according to the formula $I_x = i + \omega\,(\mathcal{J}_o + \omega^2\mathcal{J}_1)$. The higher order term is included to account for the increase of the moment of inertia due to the gradual loss of pairing correlations and centrifugal stretching.

We observe in fig. 4 that I_x increases almost linearly as a function of the frequency for $\hbar\omega > 0.37$ MeV, which implies that at the higher frequencies the higher order term in the expansion of I_x is very small for all the rotational bands observed. This is not as spectacular an effect as observed for ^{168}Hf [7] and ^{168}Yb [8], but very similar to

what has been observed in ^{165}Yb [9]. The situation is somewhat different for ^{164}Yb (fig. 5), where small non linear terms are still needed in the expansion of I_x. Nevertheless we observe that the slopes of the I_x versus $\hbar\omega$ plot are almost identical for both isotopes at the higher frequencies. The increase of I_x for the last point in the yrast sequence in ^{164}Yb might correspond to the beginning of the proton crossing which is theoretically predicted around $\hbar\omega_c = 0.5$ MeV.

The kinematic moment of inertia, $J^{(1)} = I_x/\omega$, can be expressed as $\mathcal{J}^{(1)}(\omega) = i/\omega + \mathcal{J}_0 + \omega^2\mathcal{J}_1$ and has been plotted as a function of the frequency for both isotopes in fig. 6. The same features as observed in the $I_x(\omega)$ plots are present : For ^{163}Yb, $\mathcal{J}^{(1)}(\omega)$ is almost constant at the highest frequencies, with a slight decrease for the yrast band. It should be noticed that $\mathcal{J}^{(1)}$ remains essentially constant at high frequencies for the range of neutron numbers between ^{163}Yb and ^{168}Yb although an $A^{5/3}$ dependence would imply a 5% increase.

In order to compare the experimental data to the predictions of the C.S.M.[10], the excitation energies E' and aligned angular momenta I_x should be expressed in the rotating frame which requires the choice of an appropriate parametrized reference. We first used an yrast V.M.I. reference ($\mathcal{J}_0 = 32.5\ \hbar^2\ MeV^{-1}$ and $\mathcal{J}_1 = 62.5\ \hbar^4\ MeV^{-3}$ for ^{163}Yb, $\mathcal{J}_0 = 23\ \hbar^2\ MeV^{-1}$ and $\mathcal{J}_1 = 90\ \hbar^4\ MeV^{-3}$ for ^{164}Yb) as presented in fig. 7.

In ^{164}Yb the S-band crosses the ground state band at $\hbar\omega = 0.25$ MeV with a gain in alignment $\Delta i = 8\ \hbar$ as predicted by the C.S.M. for the AB crossing. As has been observed previously in ^{162}Yb [11] the extension of the ground state band is found to make a further crossing at $\hbar\omega = 0.35$ MeV with a gain of alignment in excess of 8 $\hbar$. This is larger than the alignment gain at the first crossing and suggests that the second crossing corresponds to the alignment of four quasineutrons (ABCD).

The $(-,o)_1$ band is seen to gain 4 $\hbar$ in alignment at $\hbar\omega = 0.30$ MeV and is interpreted as the crossing of the two quasineutron band (AF) and the four quasineutron band (AFBC). The $(-,0)_2$ band observed in this and earlier [6] experiments might be identified with the configuration BE. The (-,1) band is seen to gain alignment gradually with increasing $\hbar\omega$. It has been suggested that this band has octupole vibrational character at low frequencies and gradually aquires two quasineutron

properties with increasing frequency [6]. A two to four quasineutron crossing is not obviously apparent in the data but presumably occurs at $\hbar\omega \sim 0.3$ MeV.

In ^{163}Yb negative parity bands of signature +1/2 and -1/2 are both seen to make crossings at $\hbar\omega = 0.23$ MeV. The (+,1/2) band is observed to have a crossing at $\hbar\omega = 0.35$ MeV and is identified with the configuration change A → ABC.

Since the I_x versus $\hbar\omega$ plots were observed to be almost linear at the higher frequencies we have also expressed the energy (routhians) and alignments in the C.M.I. frame as shown in fig. 8 and fig. 9. The value $\mathcal{J} = \mathcal{J}_o = 61.5\ \hbar^2\ \text{MeV}^{-1}$ which corresponds to $\mathcal{J}_{ref} = 1.22\text{x}10^{-2}\ A^{4/3}$ for A = 164 was used and is also the mean value obtained from the I_x v.s. $\hbar\omega$ slopes in both isotopes. It is interesting to notice that in this common reference frame the relative alignments are almost the same for ^{163}Yb and ^{164}Yb at the highest frequencies. At such frequencies the even A nucleus has bands with seniority two character (two quasineutrons aligned) while for the odd-A system the seniority is three. Similar alignments expressed relative to the same reference in both cores suggest that the pairing in the odd-A nucleus is significantly smaller than for the even-A nucleus.

We can see in fig. 9 that the positive parity state $(\pi,\alpha) = (+,+)$ remains yrast up to frequencies $\hbar\omega = 0.5$ MeV as observed in ^{167}Yb [11] (and in ^{161}Yb up to the observed frequency $\hbar\omega = 0.4$ MeV). Conversely, in the other isotopes ^{165}Yb [9] and ^{169}Yb [12] the negative parity band $(\pi,\alpha) = (-,+)$ becomes the yrast state at the higher frequencies. This neutron number dependance of the single-neutron states energy sequences has been interpreted as an evidence for the disappearence of the neutron pairing correlations [12].

III - A NON-COLLECTIVE ROTOR : ^{154}Er

The previously described nuclei ($N \geqslant 90$) are deformed prolate rotors generating high angular momentum by rotating around an axis perpendicular to the symmetry axis.

Conversely in a weakly deformed oblate-shape nucleus near to closed shells such as ^{154}Er which has 4 neutrons and 4 protons outside the doubly closed shells N = 82, Z = 64, large angular momentum can be generated as successive high-j single particles align their spins along the symmetry axis.

The ^{154}Er nucleus is inside the island of high spin isomers which had been observed in the vicinity of the double shell closure with relatively long deexcitation times compared to 1ps[13].

^{154}Er was produced by using the reaction $^{118}Sn(^{40}Ar,4n)$ with a 175 MeV beam from the 88-inch cyclotron of the Lawrence Berkeley Laboratory. The data were taken with the twelve first Compton-suppressed Ge detectors of the Berkeley array which is now completed to twenty one detectors. A ^{118}Sn lead-backed target was used. No appreciable Doppler broadening of the γ-rays was observed up to 1400 keV indicating that the observed decay was proceeding through high spins of at least picosecond half-lives.

In this experiment about $150x10^6$ double and $24x10^6$ triple events were recorded. Such a statistics for triples is about what is generally obtained for doubles in conventional experiments, and allows a new fruitful analysis of the coincidence data. We can then create a γ-γ matrix with the requirement that all points are in coincidence with a specific transition and gate again across this matrix after subtraction of a relevant background matrix. Such a technique may compensate to some extent the absence of a Total Energy/Multiplicity filter by selecting in a different way a specific reaction channel. A gate on the 924 keV $(34^+ \rightarrow 33^-)$ transition obtained in the double data is shown in fig. 10a. An example of a triple coincidence spectrum is shown in fig. 10b with a double gate on the 560 + 561 keV transitions which shows evidence for a third 562 keV transitions.

The ^{154}Er nucleus decay has been studied by different groups [14,15,16] with a number of discrepancies in the higher spins level ordering. The level scheme obtained in this work is shown in fig. 11 and appears to be closer, up to $I^\pi = 33^-$, to the one obtained by the Orsay-Strasbourg collaboration [16]. It is somewhat preliminary since a number of weak transitions has not yet been placed. The spins are based on angular correlations and the higher ones are only tentative.

The 11^- isomer is also observed in other N = 86 isotones ^{152}Dy [17,18,19] and ^{156}Yb [20]. The isomeric transitions deexciting this state to the 9^- and 10^+ levels had not been observed and were assumed to have very low energies. We could observe in the coincidence data a 135 keV transition (and tentatively a very weak 226 keV transition) connecting the higher levels of the negative parity sequence above the isomer to the continuation of the ground state band. It was then possible to deduce the energy of both isomeric transitions Δ = 11 keV and Δ' = 9 keV.

The decay of ^{154}Er is characteristic of nuclei with a few nucleons outside of closed shells with an irregular multiparticle-hole deexcitation pattern. Weak oblate deformation is expected at high spins, the total angular momentum being aligned with the symmetry axis.

A partial level scheme above the 11^- isomer is shown in fig.12 together with the interpretation by Dudek[16,21] using the deformed Wood-Saxon potential with the modified Strutinsky prescription[22]. The theoretical decay pattern is based on the lowest energy minimization principle, and such calculations were already used to intrepretate a recent level scheme of ^{154}Er[16] which is very similar to what was found in this work up to $I^\pi = 33^-$.

The high energy part above $I^\pi = 33^-$ is displayed with more details in fig. 13 together with the calculated decay scheme[21].

A recent g-factor measurement of the 11^- isomeric state[23] is in agreement with an aligned two neutrons configuration $\nu(h9/2, i13/2)$ and supports the $I^\pi = 11^-$ assignment.

The $I^\pi = 17^-$ and 33^- states correspond to maximum alignment states within their configuration. The 33^- state decays through both positive and negative parity paths. The $I^\pi = 27^- \rightarrow 33^-$ negative parity sequence can be compared to the $I^\pi = 11^- \rightarrow 17^-$ sequence ; according to the theoretical calculations then both correspond to rearrangements in the neutron ($f_{7/2}$) multiplet. The $11^- \rightarrow 17^-$ sequence built on the 11^- isomer is very similar in ^{152}Dy[19], ^{154}Er and ^{156}Yb[20] and seems to be characteristic of N = 86 isotones. The positive parity path decays through the 279 and 562 keV transitions which were assigned as E1 by linear polarization measurements[16]. The most likely theoretical prediction corresponds to the configuration $\pi(d^{-1}_{5/2}, h^5_{11/2})$ involving the excitation of a proton-hole over the Z = 64 energy gap.

The 36 state at 11.896 MeV decays to the 33^- state via the three dipole transitions 394, 150 and 924 keV. The first predicted 36^- state would be 2 MeV above. The first predicted 36^+ state corresponds to the maximum aligned configuration $\nu(i^2_{13/2})^{max}_{12} \otimes \nu(f^2_{7/2}, h_{9/2})^{max}_8 \otimes \pi(h^4_{11/2})^{max}_{16}$. Weak transitions of energy higher than 1 MeV feed the 36 state. As shown in fig. 13, the calculated states above I = 36$\hbar$ involve proton over-the-Z = 64 gap or neutron over-the-N = 82 gap transitions which seem to be the easiest way to gain high angular momentum at such spins.

Cranking Shell Model calculations with the deformed Woods-Saxon potential [16,24] predict that ^{154}Er should remain oblate up to spin I ~ 44-46h where an "oblate-triaxial" shape coexistence near the yrast line is expected. The superdeformed minimum should become yrast for spins I ~ 78h, but should already be formed below I ~ 50h. The relative energy between the superdeformed band and the yrast configuration is expected to decrease quickly with increasing spin and one might expect that the superdeformed band develops down to rather low spin values. A study of the E_γ-E_γ correlations of ^{154}Er at spins I > 40ħ would be particularly interesting.

IV - The "Chateau de Cristal" and its use as an Anti-Compton array

We shall here briefly describe the main characteristics of the "Chateau de Cristal" (Crystal Castle) national french 4 π-γ array which will be operating in middle of 1985 [25].

In all the existing multi-detectors arrays with Anti-Compton shields, the Compton suppression material and inner core are made of NaI or BGO elements.

The production of large BaF2 crystals have been recently developped [25]. Table I gives the main characteristics of BaF2 as compared with NaI and BGO. We can see there that both the energy resolution and density of BaF2 are intermediate between those of NaI and BGO. For example a 1 MeV γ-ray will be 95% absorbed in 6cm thick BGO, 10.5 cm BaF2 and 14 cm NaI. The very interesting property of BaF2 is the existence, besides the slow light component at 325 nm (τ = 620ns), of a fast component at 220 nm (τ ~ 0.6ns) in the ultraviolet, allowing a very good timing, comparable to that of plastic scintillators.

Table I
Comparison of different scintillation materials

Material	Wavelength of maximum emission (nm)	Decay constant (ns)	Density (kg/m^3)	Hygroscopic	Resolution (1 MeV γ-rays) Energy	Time
NaI	410	230	3.67	yes	7-8 %	~ 3ns
BGO	480	300	7.13	no	~15 %	~ 4ns
BaF2	slow 325 fast 220	620 0.6	4.88	no	~10%	~0.6ns

Because of those interesting characteristics (and much lower cost than BGO) BaF2 was the material choosen for the construction of the "Chateau de Cristal". The french 4 π-γ array will comprise (in the first stage) 74 hexagonal BaF2 detectors (Ø = 10cm, L = 14cm) arranged in the geometry indicated in fig. 14 (it might be extended up to 122, 182... detectors). The hexagonal modular structure of the "Chateau de Cristal" allows to associate it to Ge detectors in order to create an Anti-Compton device. A Ge detector can be shielded with 5 BaF2 elements plus a small additional backscatter BaF2 detector (fig.15). Therefore, at the cost of some supplementary elements the "Chateau de Cristal" can be transformed into a 38 elements core surrounded by 12 Ge detectors with Anti-Compton shields (six on each side of the reaction plane) as indicated in fig. 15. The Ge detectors will then be at d = 26.5cm from the target (it would also be possible to use other configurations such as 12 Ge detectors at d = 16.5cm from the target with a remaining 14 detectors inner core).

The existence of the fast light component of BaF2 will allow a very good neutron discrimination. Furthermore it will be possible to select a specific range of spins located above or below nanosecond isomeric states.

The good properties of BaF2 combined with a versatile construction allows to use the "Chateau de Cristal" array wether as a conventional 4 π-γ array or as a Compton suppressed Ge array with a smaller core. The use of BaF2 detectors for γ-ray spectroscopy with excellent timing properties will provide a new exciting tool for γ spectrometry.

CONCLUSION

We have presented some results obtained for nuclei located in different deformation regions for which the TESSA2 and Berkeley array are respectively the best existing spectrometers for discrete lines γ-spectrometry. The french national array under construction has been shortly described.

We gratefully thank J. Dudek for communicating his calculations for the interpretation of the high spin states of ^{154}Er.

REFERENCES

(1) Twin P.J., Proceed. of the Intern. Conf. on Nuclear Physics, Florence II (1983) 527.
Twin, P.J., Nolan P.J., Aryaeinejad R., Love D.J.G., Nelson A.H. and Kirwan A., Nucl. Phys. A409, 343C (1983).

(2) Twin P.J., Proceed. of the Conf. on Instrumentation for Heavy Ion Nuclear Research, Oak-Ridge (November 1984).

(3) Diamond R.M. and Stephens F.S., The high Resolution Ball, unpublished, Berkeley (1983).
Stephens F.S., Proceed. Conf. on High Angular Momentum Properties of Nuclei, Oak-Ridge (1982) 479 and Proceed. Intern. Symposium on In-Beam Nuclear Spectroscopy, Debrecen (May 1984).

(4) Bengtsson T., Private communication (1985).

(5) Kownacki J., Garrett J.D., Gaardhøje J.J., Hagemann G.B., Herskind B., Jonsson S., Roy N., Ryde H. and Walus W., Nucl. Phys. A394, 269 (1983)

(6) Jonsson S., Roy N., Ryde H., Walus W., Kownacki J., Garrett J.D., Hagemann G.B., Herskind B., Bengtsson R. and Aberg S., Lund-NBI preprint (1985).

(7) Chapman R., Lisle J.C., Mo J.N., Paul E., Simcock A., Wilmott J.C. Leslie J.R., Price H.G., Walker P.M., Bacelar J.C., Garrett J.D., Hagemann G.B., Herskind B., Holm A. and Nolan P.J., Phys. Rev. Lett. 51, 2265 (1983).

(8) Lisle J.C., Proc. of the 5th Nordic Meeting on Nucl. Phys. Jyväskylä (1984) 45.

(9) Schück C., Bendjaballah N., Diamond R.M., Ellis-Akovali Y., Lindenberger K.H., Newton J.O., Stephens F.S., Garrett J.D. and Herskind B. Phys. Lett. 142B, 253 (1984).

(10) Bengtsson R. and Frauendorf S., Nucl. Phys. A327, 139 (1979).

(11) Gaardhøje J.J., Thesis Risø (1980).
Garrett J.D., Hagemann G.B. and Herskind B., Private communication.

(12) Garrett J.D., Workshop on Nucl. Collective States, Suzhou, China (1983) and to be published.
Bacelar J.C., Diebel M., Ellegaard C., Garrett J.D., Hagemann G.B., Herskind B., Holm A., -X.Yang C., Tjøm P.O. and Lisle J.C., Proc. of the 5th Nordic Meeting on Nucl. Phys. Jyväskylä (1984) 201.

(13) Pedersen J., Back B.B., Bernthal F.M., Bjornholm S., Borgreen J., Christensen O., Folkmann F., Herskind B., Khoo T.L., Neiman M., PühlHofer F., Sletten G., Phys. Rev. Lett. 39, 990 (1977).

(14) Aguer P., Bastin G., Thibaud J.P., Barnéoud D., Boutet J., Foin C., Z. Phys. A285, 59 (1978).
Aguer P., Bastin G., Charmant A., El-Masri Y., Hubert P., Janssens R., Michel C., Thibaud J.P., Vervier J., Phys. Lett. 82B, 55 (1979).

(15) Baktash C., Mateosian E.der, Kistner O.C., Sunyar A.W., Phys. Rev. Lett. 42, 637 (1979).

(16) Beck F.A., Dudek J., Haas B., Merdinger J.C., Nourreddine A., Schutz Y., Vivien J.P., Hubert Ph., Dassié D., Bastin G., Nguyen L. Thibaud J.P., Nazarewicz W., Z. Phys. A319, 119 (1984).

(17) Khoo T.L., Smither R.K., Haas B., Häusser O., Andrews H.R., Horn D. Ward D., Phys. Rev. Lett. 41, 1027 (1978).

(18) Merdinger J.C., Beck F.A., Byrski T., Gehringer C., Vivien J.P., Bozek E., Styczen J., Phys. Rev. Lett. 42, 23 (1979).

(19) Styczen J., Nagai Y., Piiparinen M., Ercan A., Kleinheinz P., Phys. Rev. Lett. 59, 1752 (1983).

(20) Lister C.J., Horn D., Baktash C., Mateosian E.der, Kistner O.C., Sunyar A.W., Phys. Rev. C23I, 2078 (1981).

(21) Dudek J., private communication (1985).

(22) Dudek J., Szymanski Z., Werner T., Faessler A., Lima C., Phys. Rev. C26, 1712 (1982).

(23) Nguyen L., Sergolle H., Aguer P., Auger G., Bastin G., Lönnroth T., Thibaud J.P., Thomé L., Z. Phys. A309, 207 (1983).

(24) Dudek J. and Nazarewicz, Phys. Rev. C31, 298 (1985).

(25) Vivien J.P., C.R.N. annual report Strasbourg (1982).
Beck F.A., Proceed. of the Conf. on Instrumentation for Heavy Ions Nuclear Research, Oak-Ridge (November 1984).

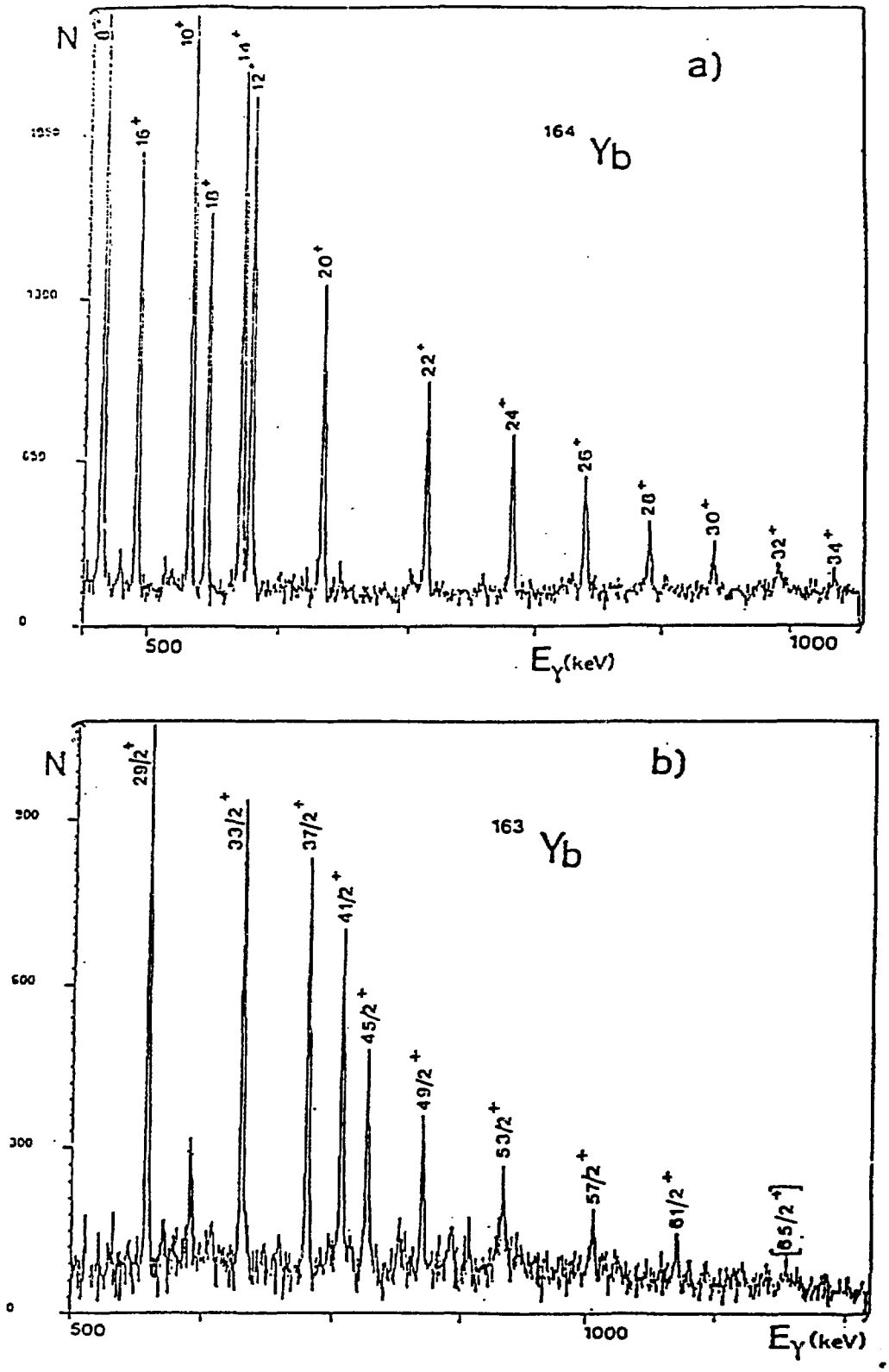

Fig. 1 - Gamma-gamma coincidence spectra corresponding to the sum of the higher γ gates in the yrast lines of ^{164}Yb and ^{163}Yb obtained by using total energy and multiplicity gates on the BGO inner ball to preferentially select the 4n and 5n reactions (a) and b) respectively).

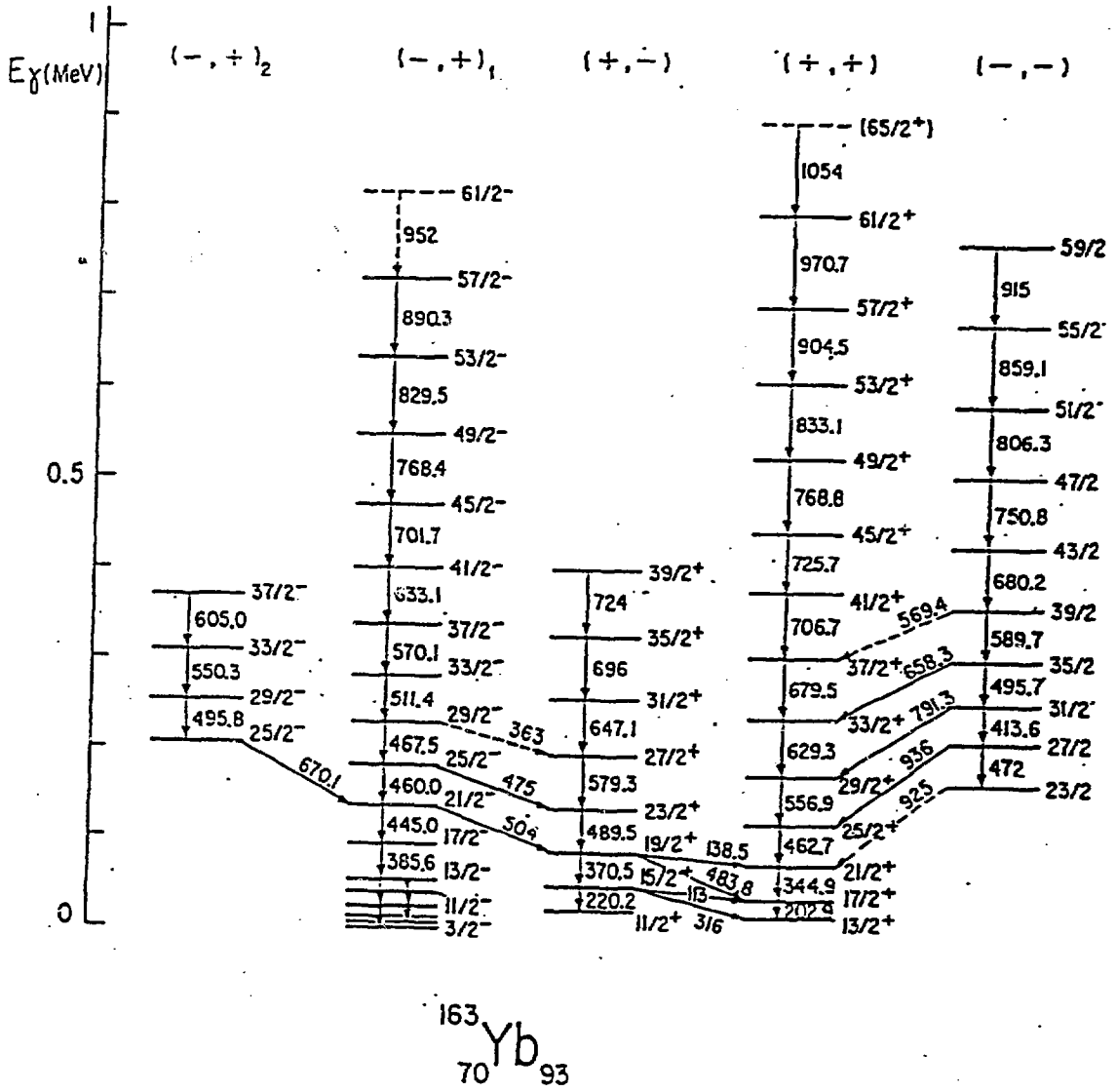

$^{163}_{70}Yb_{93}$

Fig. 2 - High spin level scheme of ^{163}Yb obtained in the present work.

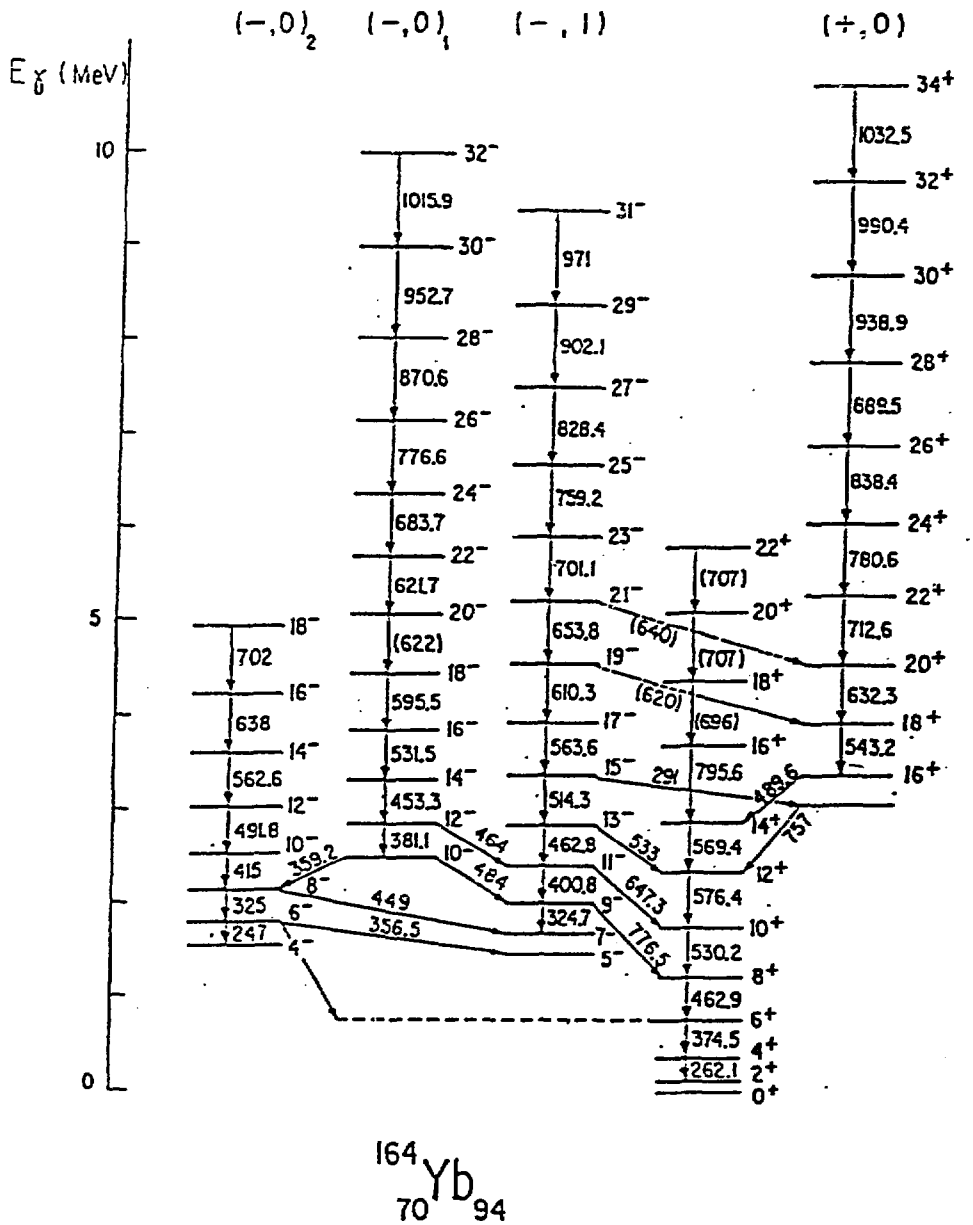

Fig. 3 - High spin level scheme of ^{164}Yb obtained in the present work.

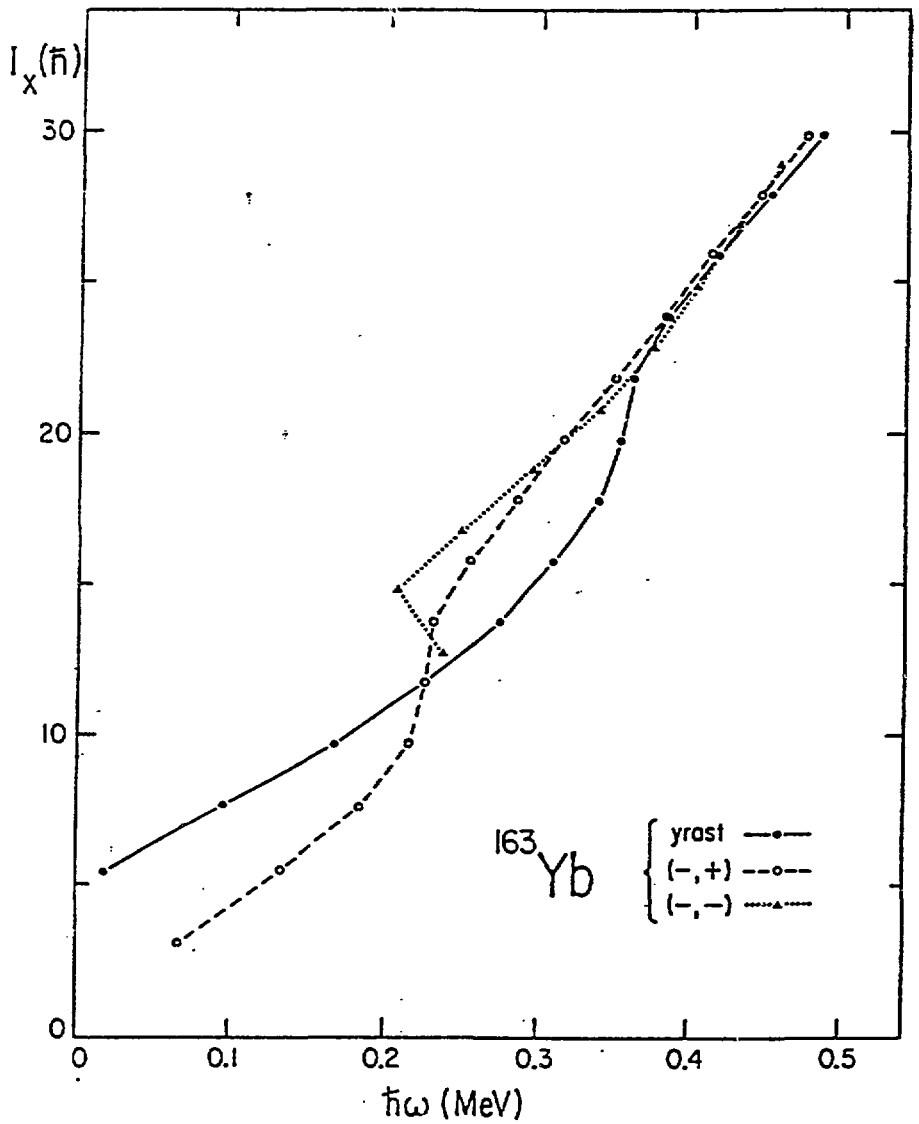

Fig. 4 - Experimental I_x versus $\hbar\omega$ plots for three different configurations in ^{163}Yb.

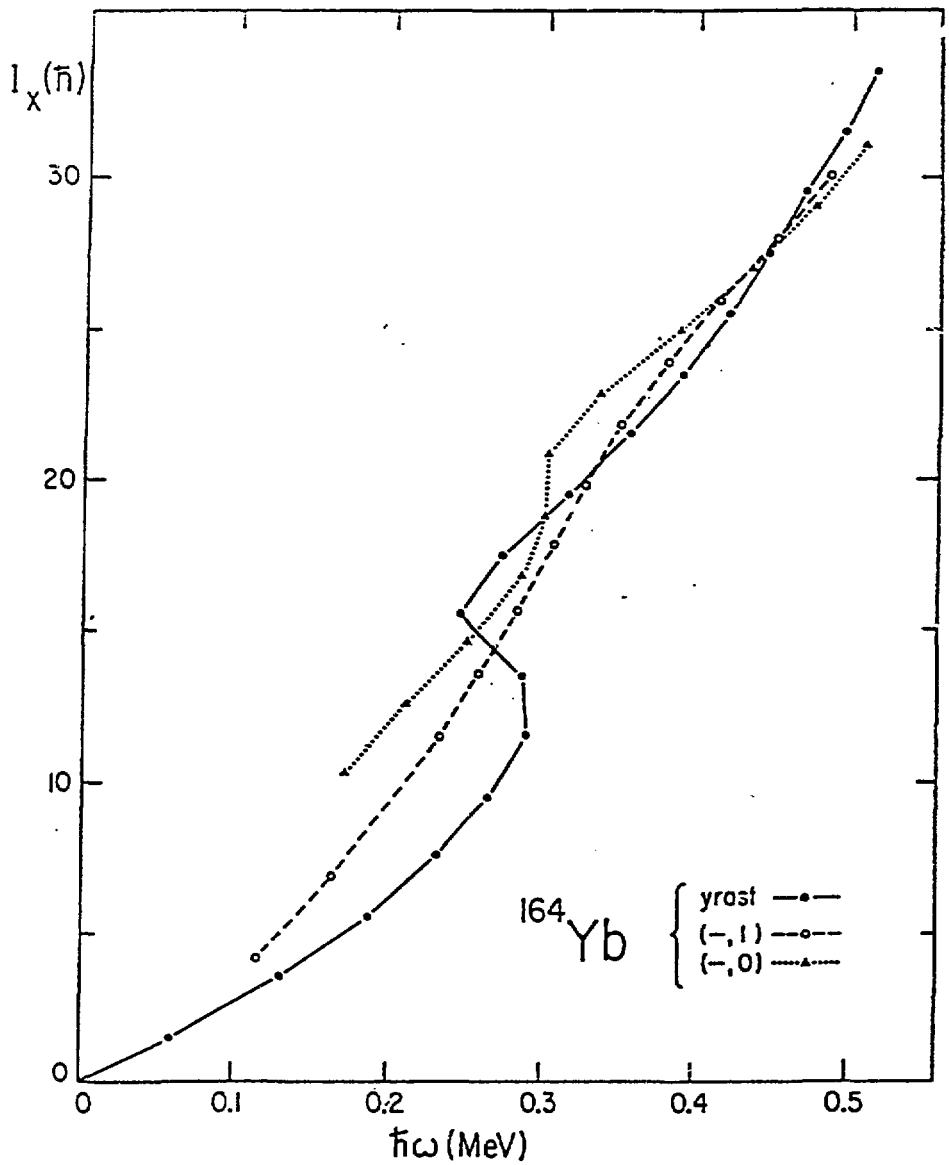

Fig. 5 - Experimental I_x versus $\hbar\omega$ plots for three different configurations in ^{164}Yb.

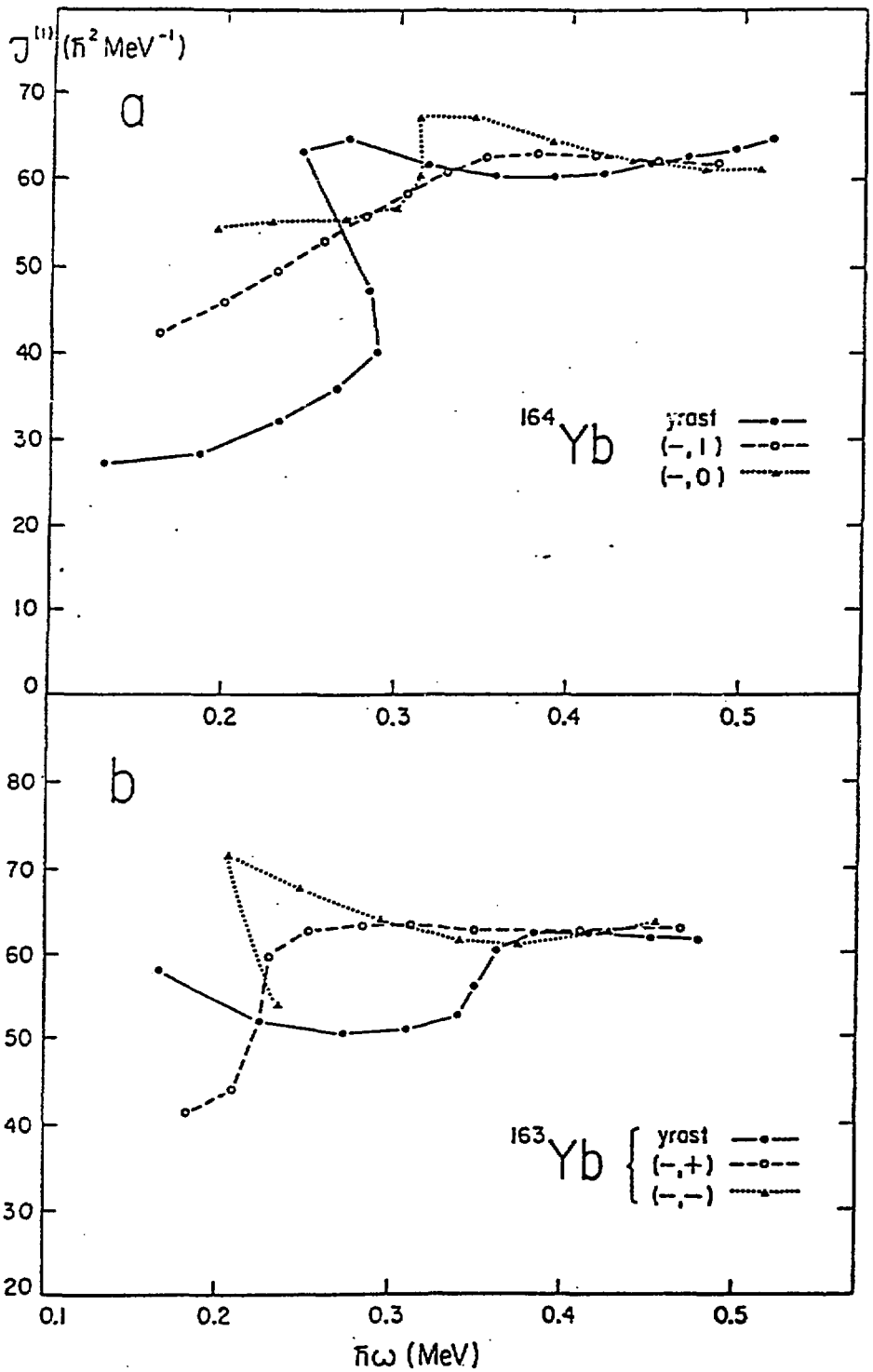

Fig. 6 Kinematic moment of inertia for different rotational configurations in ^{164}Yb and ^{163}Yb respectively.

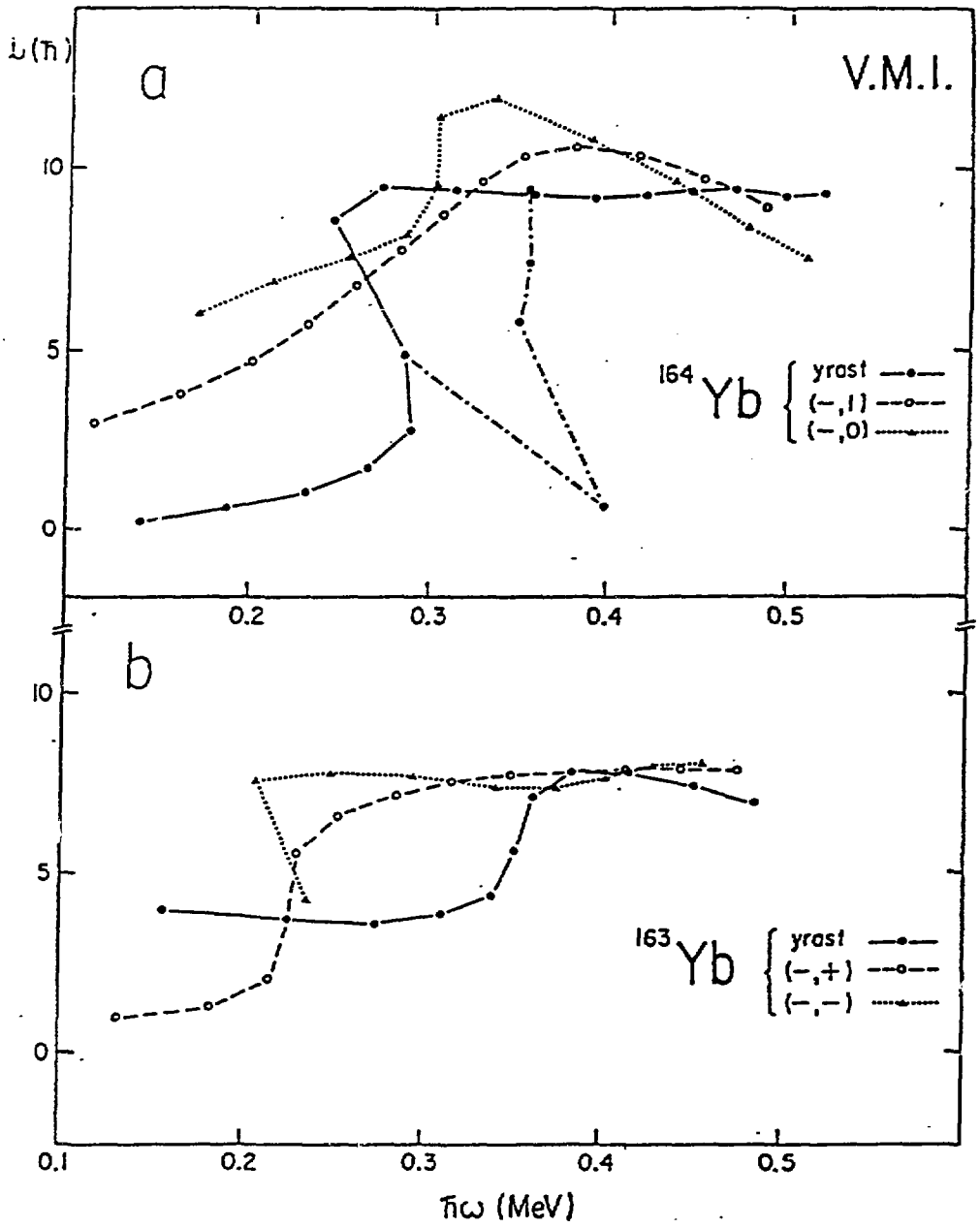

Fig. 7 - a) Experimental alignment as a function of $\hbar\omega$ for different configurations in ^{164}Yb obtained by using a V.M.I. reference $J = \omega J_o + \omega^3 J_1$ with $J_o = 23\hbar^2$ MeV^{-1} and $J_1 = 90\hbar^4$ MeV^{-3}.
b) Experimental alignment as a function of $\hbar\omega$ for different configurations in ^{163}Yb in the V.M.I. reference with $J_o = 32.5\hbar^2$ MeV^{-1} and $J_1 = 62.5\hbar^4$ MeV^{-3} for ^{163}Yb.

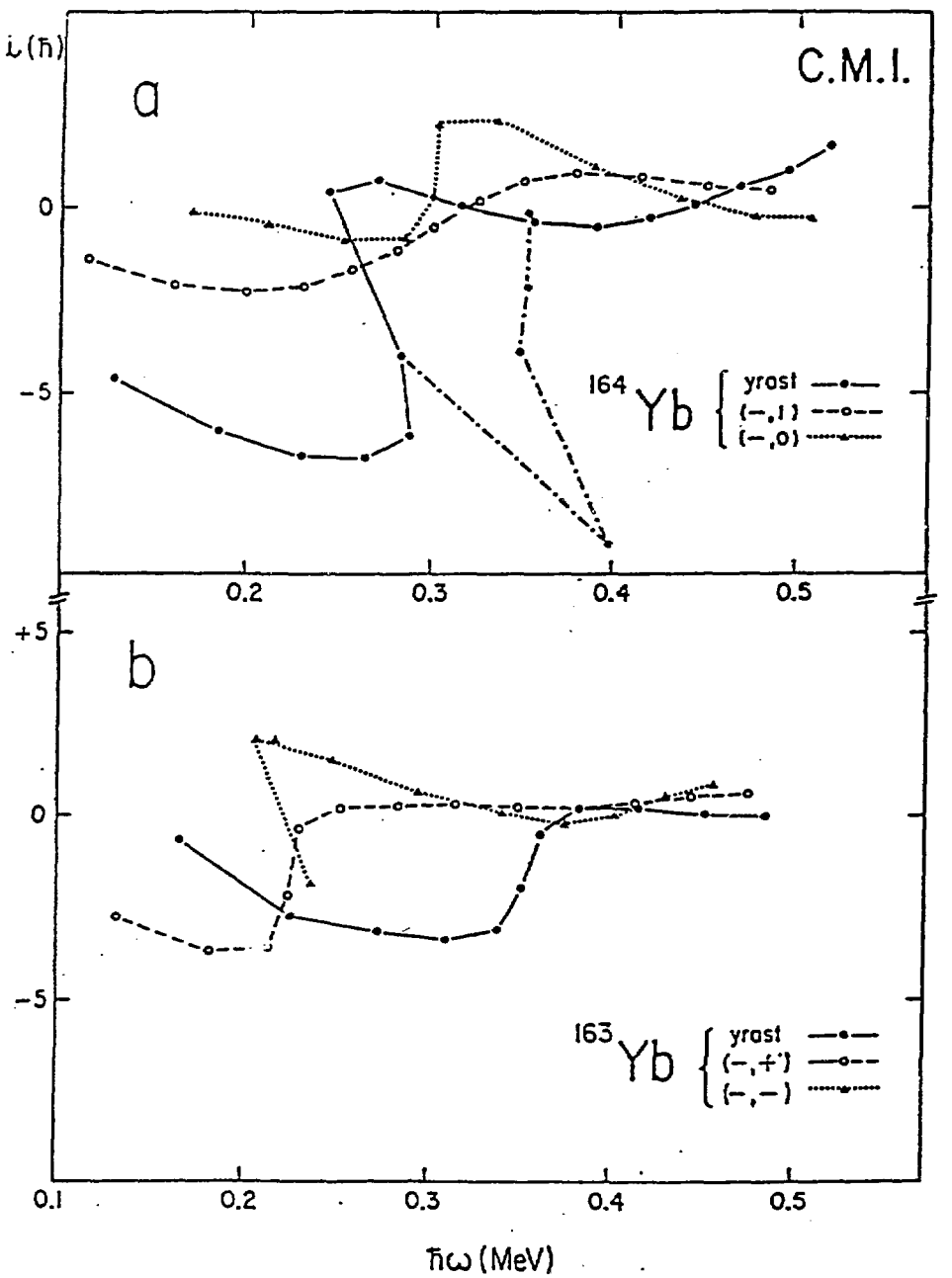

Fig. 8 - Experimental alignment versus $\hbar\omega$ plots for ^{164}Yb and ^{163}Yb respectively, obtained by using the same C.M.I. reference with $\mathcal{J} = \mathcal{J}_o = 61.5\ \hbar^2 MeV^{-1}$.

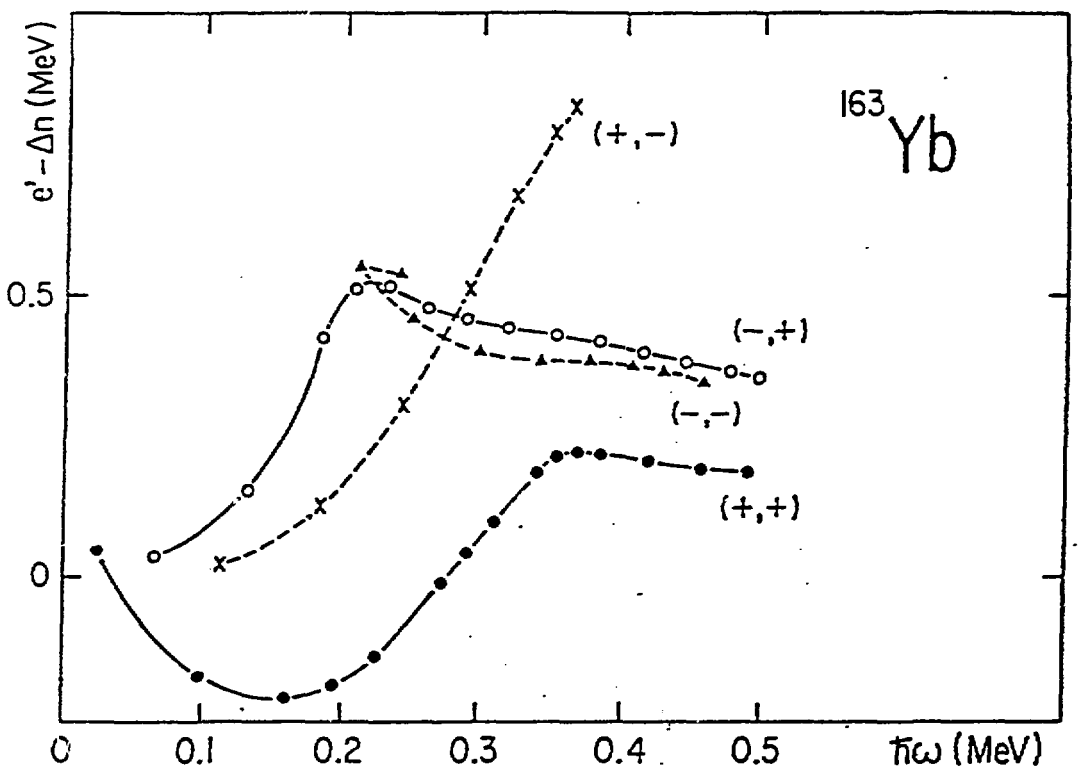

Fig. 9 - Experimental routhians in the C.M.I. reference ($\mathcal{J} = \mathcal{J}_0 = 61.5\hbar^2 MeV^{-1}$) for different configurations in ^{163}Yb.

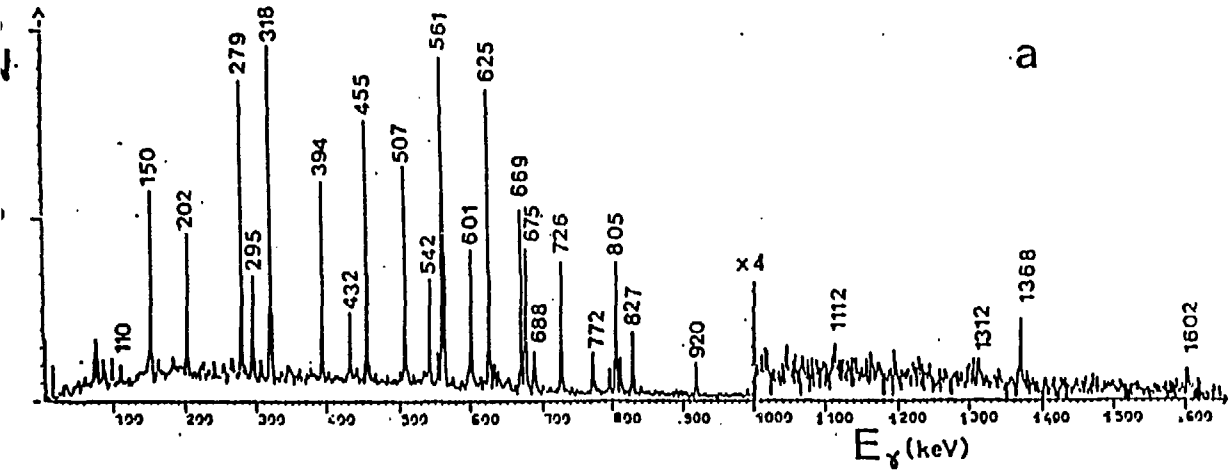

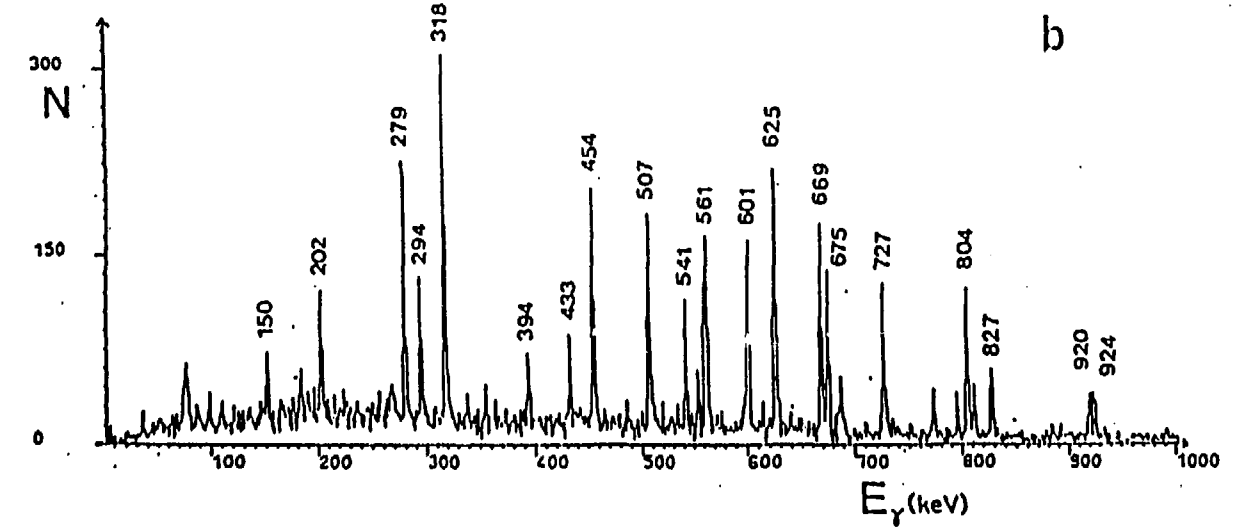

Fig. 10

a) Spectrum from the double coincidences data of ^{154}Er with a gate on the 924 keV transition ($34^+ \rightarrow 33^-$).

b) Spectrum from the triple coincidences data of ^{154}Er with a double 560+561 keV gate.

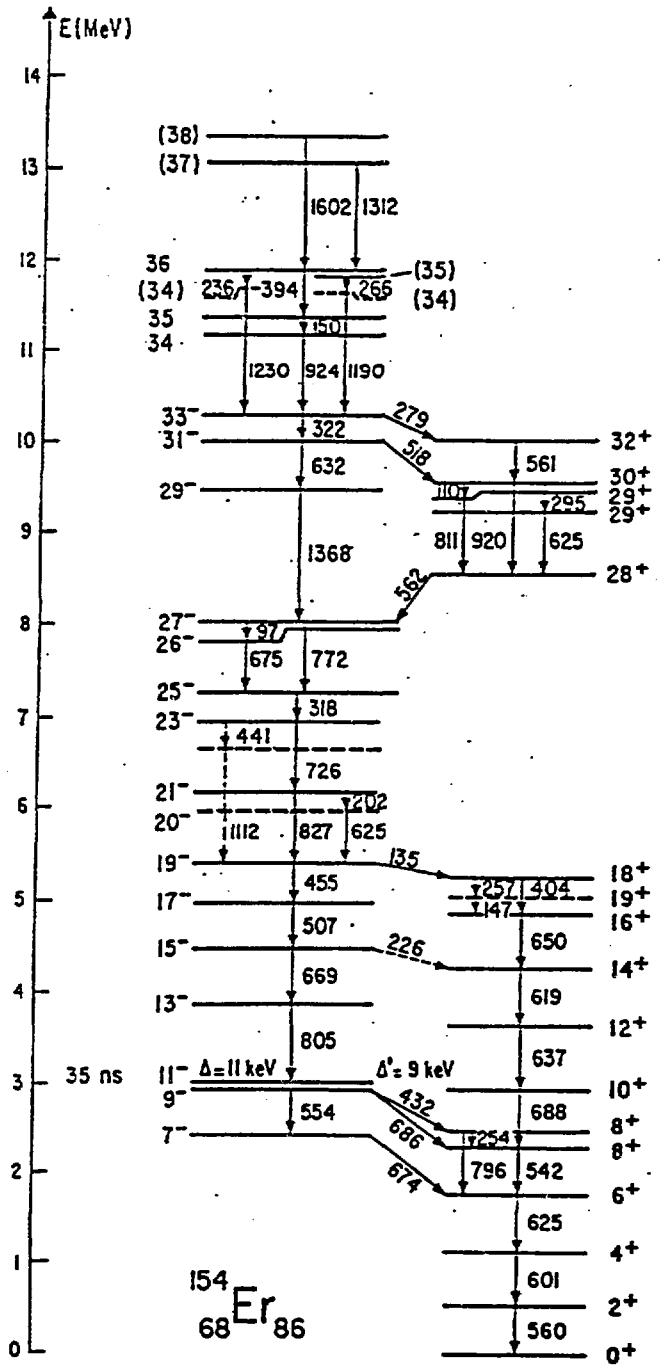

Fig. 11 - Level scheme of ^{154}Er as obtained in the present work. The ordering of the levels marked with dotted lines in uncertain.

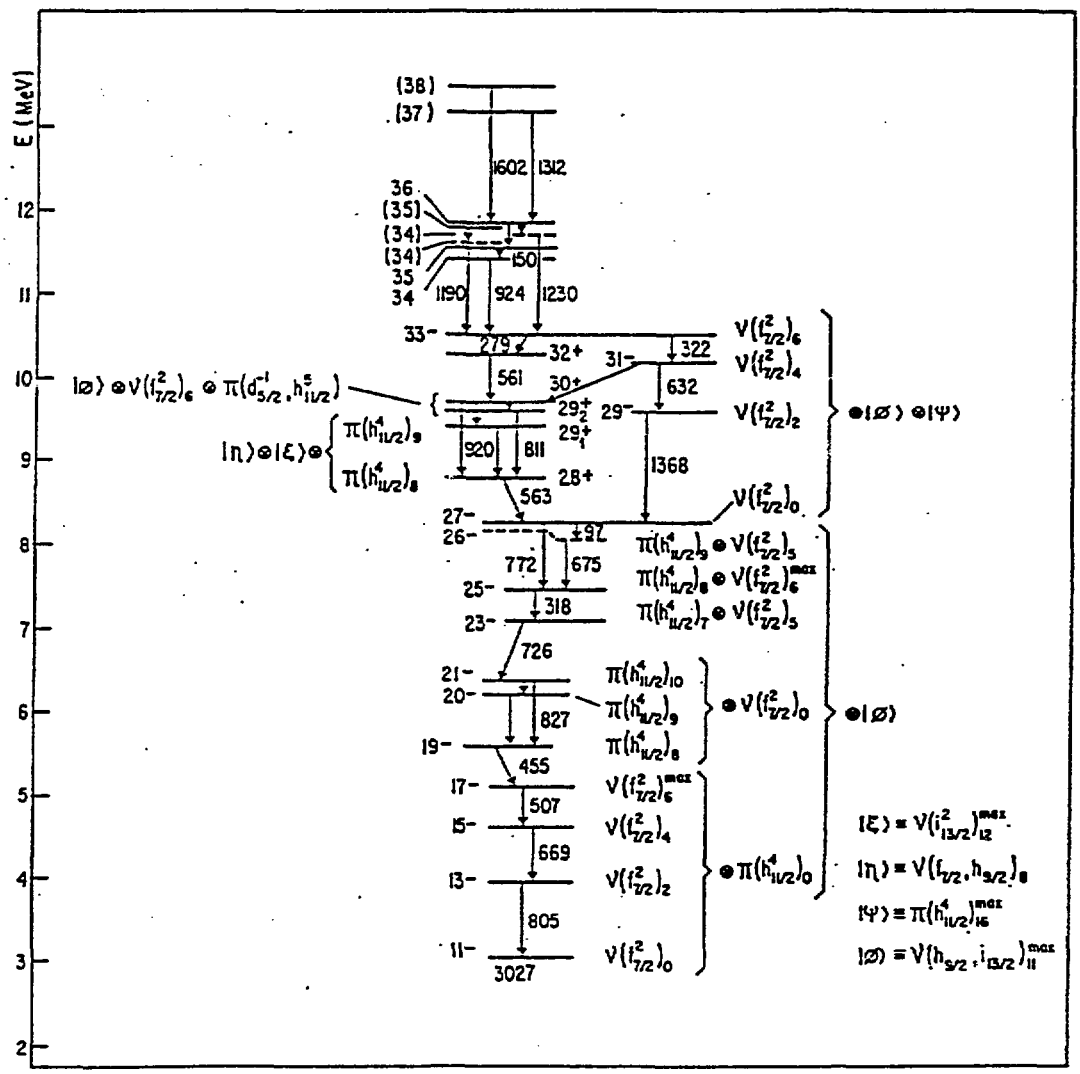

Fig. 12 - Partial high spin level scheme of ^{154}Er above the 11^- isomer together with the theoretical single particle orbitals interpretation[16,21].

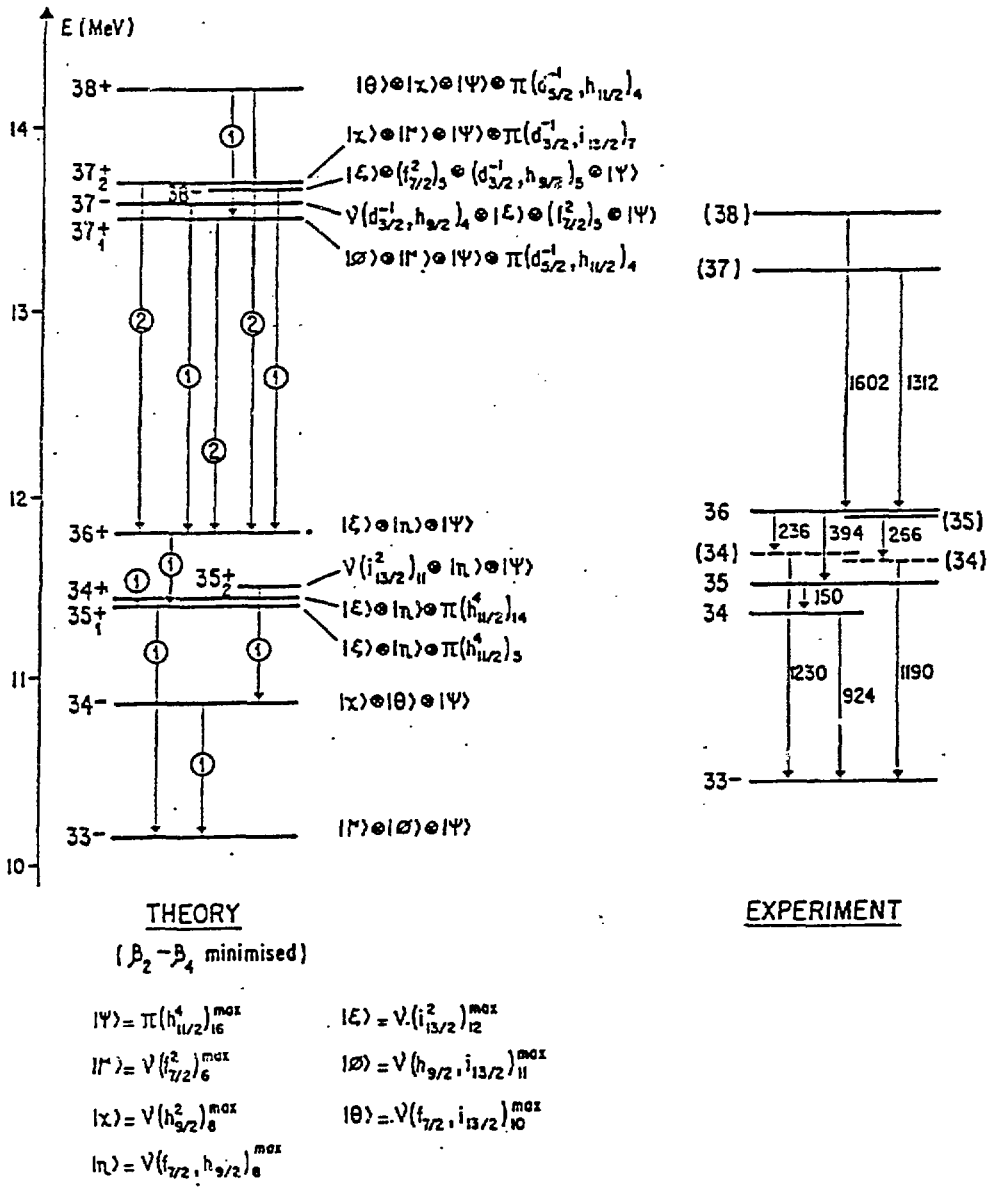

Fig. 13 – Comparison between the experimental and calculated[21] decay scheme above the 33^- state. The numbers inside the circles correspond to the number of particles rearrangement in the corresponding electromagnetic transitions.

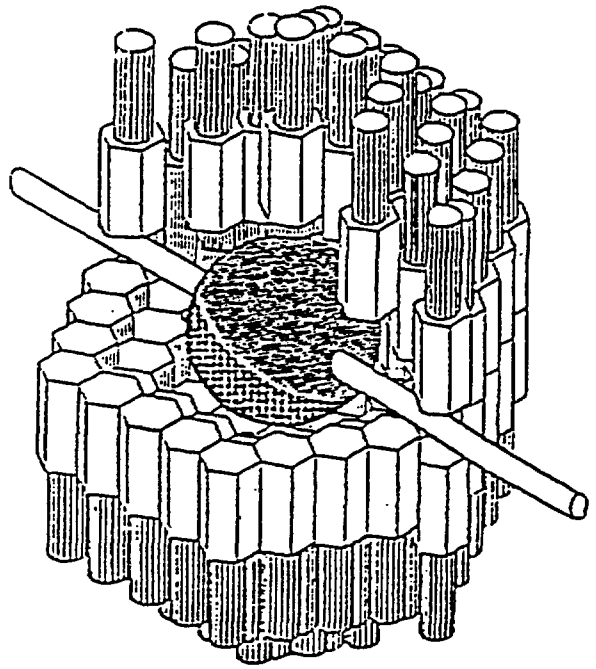

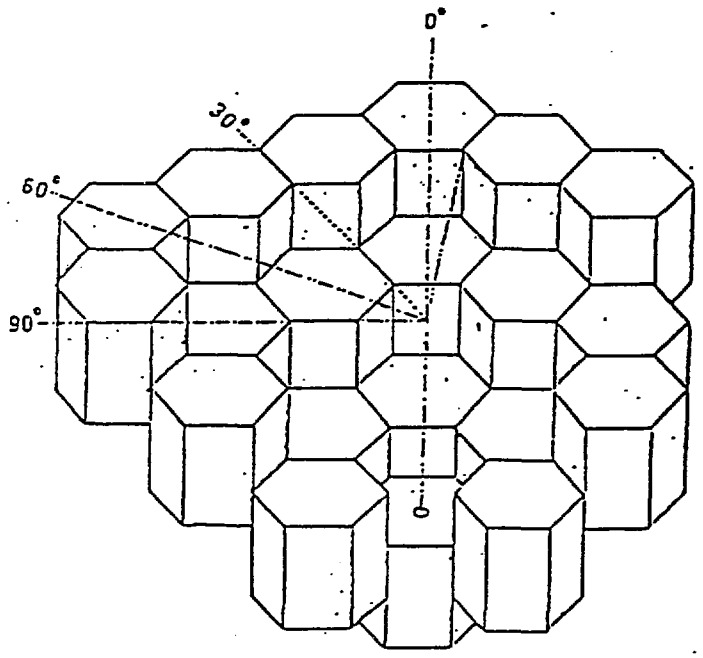

FRENCH NATIONAL BaF_2 4π-γ DETECTOR

(BORDEAUX. GRENOBLE. LYON. ORSAY. STRASBOURG)

Fig. 14 - Sketch of the "Château de Cristal" array showing
- a) partial view of the BaF2 scintillators and phototubes with the beam entrance and reaction chamber.
- b) part of the arrangement of the BaF2 crystals into six concentric rings plus two detectors.

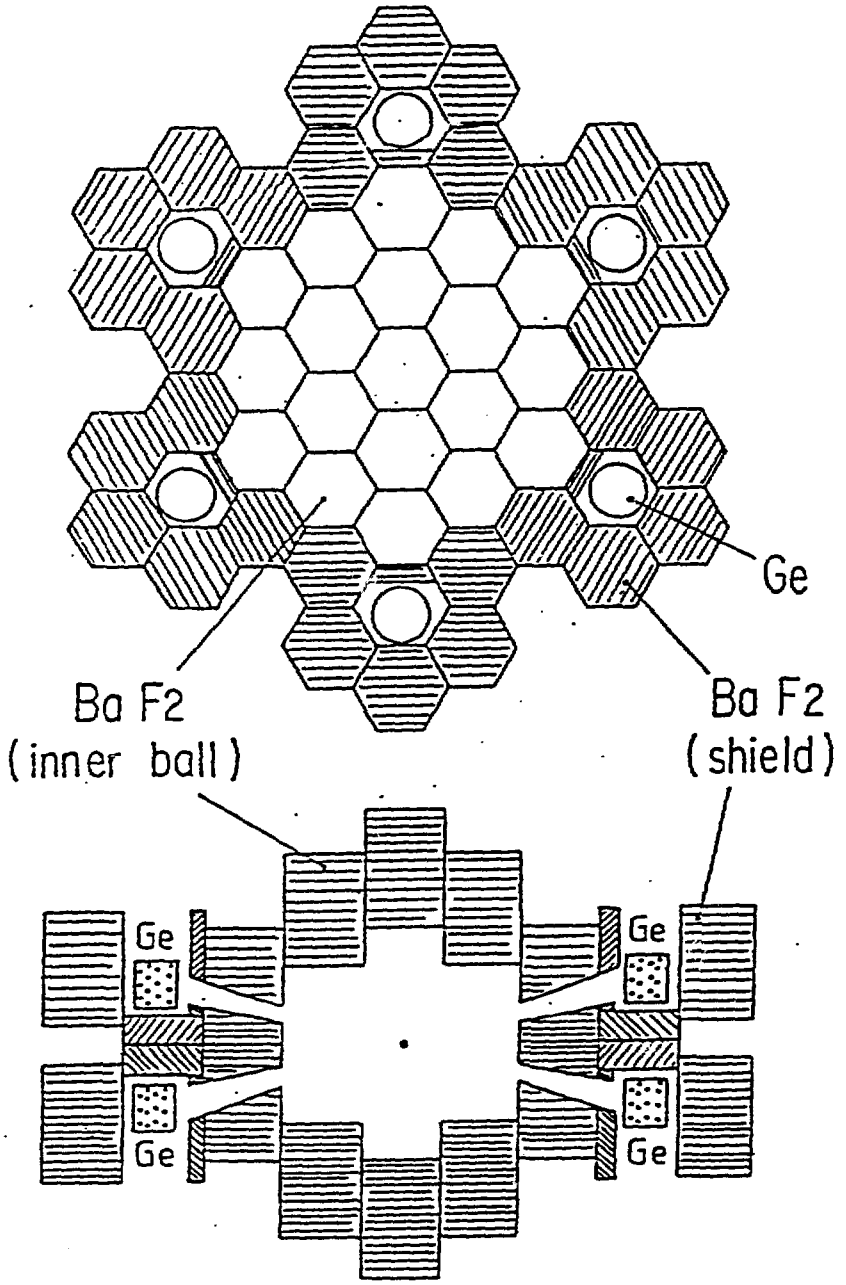

Fig. 15 - Horizontal and vertical cuts of the configuration proposed for the Compton suppressed array showing one of the two rings of six Ge detectors. Each of the twelve detectors will be surrounded by five BaF2 crystals used as a Compton-shield and an additional small hollow crystal for detecting backscattered gamma rays. The remaining 38 BaF2 detectors will be used as Sum Energy/ Multiplicity filter.